A NUMERICAL METHOD FOR REGULATING UNSTEADY FLOW IN OPEN CHANNELS

M.T.Shamaa
Irrigation & Hydraulics Dept., Faculty of Engineering, Mansoura University, Egypt

ABSTRACT

Unsteady flow problems in open channels can be classified into two types: routing and operation-type problems. In the routing problem, the Saint Venant equations is used to predict the discharge and water level in the channel during the future time series under the given conditions. On the other hand, the operation problem is used to compute the inflow at the upstream section of the channel. Also, it can be used to compute a schedule of operation for the regulating structures of the delivery system to get a predefined water demand at the downstream end of the channel. This type of problem is also known as the inverse computation of open channel flow. An explicit finite difference scheme (inverse explicit scheme) was presented to solve the operation-type problems in open channels. The inverse explicit scheme was applied to solve the Saint Venant equations based on the discretization of the Preissmann scheme. The method is numerically stable, and the computation is performed by proceeding first backward in time and then backward in space. The computed results using the inverse explicit scheme showed approximately the same accuracy as those obtained using the inverse implicit scheme [2,11] but with different values of weighting coefficients. The computed upstream discharge hydrograph by the inverse explicit scheme, when used as upstream boundary condition in the routing problem, reproduced downstream flow hydrographs very close to the predefined outflow. The implicit Preissmann scheme was used in the routing problem. The complete momentum equation was used in all the applied schemes. The finite difference inverse explicit model was successfully applied to a non-prismatic reach of El-Mansouria canal between Sanayet regulator and Bahr Tanah Canal.

INTRODUCTION

Numerical Solution of the partial differential Saint Venant equations, which express the principles of conservation of mass and momentum, can be obtained at a finite number of grid points in the rectangular spatial-time grid using finite difference methods [1,3,4,7]. Mathematical models of unsteady open channel flow are commonly built for engineering purposes[1,3,4,7,9] such as flood defence design, navigation, flood forecasting, dam-break analysis, and irrigation scheme control.

Precise control of water flow in irrigation systems is becoming very important due to increasing of water demands. Operation along irrigation canals aim to maintain a hydraulic targeted state in order to achieve reliable and equitable water deliveries to users. Mathematical models were developed for

operation-type problems [2,5,6,8,11,12] to predict the upstream inflow according to the prescribed downstream flow hydrograph.

A transient control technique, known as gate stroking [2,12], was used to set gate movements and upstream inflow according to the prescribed downstream flow hydrograph. The technique used the method of characteristics which is more complex. Easier solution for solving the unsteady open channel governing equations can be obtained using finite differences.

Two finite difference algorithms have been recently proposed for solving the inverse problem. The first one is the implicit method[2,11]and the other is the explicit method [6]. The computational scheme of the implicit method can be shown as a boundary value problem rotated 90° in the distance-time grid [2]. The specified depths and discharges at the downstream end are the initial conditions in this rotated problem and the boundary conditions can be either a discharge profile or water depth profile at both the initial time and the final computational time. The backward operation method [6] is an explicit solution based on the Preissmann scheme. In this method, the computation begins at the top-right corner of the time-distance plane, then the solution is obtained cell by cell, moving first backward in space and then backward in time.

The inverse explicit scheme, presented in this paper, can provide a more accurate solution than that obtained by the backward operation method. In this method, on the contrary of the backward operation method, the computation is performed by proceeding first backward in time and then backward in space. The inverse explicit finite difference scheme was tested with numerical experiments and was applied successfully to a non-prismatic reach of El-Mansouria canal between Sanayet regulator and Bahr Tanah canal [10].

BASIC EQUATIONS

Unsteady flow in open channels is mathematically described by a set of one-dimensional shallow water equations commonly known as the Saint Venant equations. The Saint Venant equations can be formulated in different ways, depending on the assumptions used in their derivations. Assuming no lateral outflow, these equations can be written as:

$$\frac{\partial y}{\partial t} + \frac{1}{b}\frac{\partial Q}{\partial x} = 0 \qquad (1)$$

$$\frac{\partial Q}{\partial t} + \frac{\partial}{\partial x}\left(\beta \frac{Q^2}{A}\right) + gA\left(\frac{\partial y}{\partial x} + S_f - S_0\right) = 0 \qquad (2)$$

where: A = wetted cross-sectional area; b = wetted top width; g = gravitational acceleration; Q = discharge (through A); y = depth of flow ; t = time; x = space; S_0= bottom slope of the channel and S_f = friction slope.

NUMERICAL SOLUTION METHODS

Numerical solution of the Saint Venant equations can be obtained at a finite number of grid points in the rectangular spatial-time grid using finite diff

methods [1,3,4,7]. Finite difference schemes can be classified into two types: explicit and implicit. In the explicit difference methods, the dependent variables, at a rectangular grid point on an advanced time line are determined from the known values and conditions at grid points on the present time line or present and previous time lines. In the implicit methods, unsteady flow may be obtained at a subsequent time levels on the *x-t* plane by setting up many equations as there are unknown dependent variables and by solving them simultaneously using appropriate time boundary conditions.

Preissmann Implicit Routing Model

Implicit schemes which can use large time steps without any stability problem are more widely applied. The Preissmann scheme is the most widely applied implicit finite difference method because of its simple structure with both flow and geometrical variable in each grid point [1,3,4,7]. This implies a simple treatment of boundary conditions and a simple incorporation of structure and bifurcation points. Also, it has the advantages that steep wave fronts may be properly simulated by varying the weighting coefficient.

The computational grid for the Preissmann implicit scheme is shown in Fig.1. The application of the Preissmann scheme to the derivatives in equations (1) and (2) yields:

$$\frac{\partial f}{\partial t} = \phi\frac{f_{j+1}^{n+1} - f_{j+1}^{n}}{\Delta t} + (1-\phi)\frac{f_{j}^{n+1} - f_{j}^{n}}{\Delta t} \tag{3}$$

$$\frac{\partial f}{\partial x} = \theta\frac{f_{j+1}^{n+1} - f_{j}^{n+1}}{\Delta x} + (1-\theta)\frac{f_{j+1}^{n} - f_{j}^{n}}{\Delta x} \tag{4}$$

$$f(x,t) = \theta\left[\phi f_{j+1}^{n+1} + (1-\phi) f_{j}^{n+1}\right] + (1-\theta)\left[\phi f_{j+1}^{n} + (1-\phi) f_{j}^{n}\right] \tag{5}$$

where $f_j^n = f(j\Delta x, n\Delta t)$; Δx=space interval; Δt=time interval; ϕ = a weighting coefficient for distributing terms in space and θ = a weighting coefficient for distributing terms in time, $0 \le \theta \le 1$. In the above expressions, all the variables with subscripts' n are known and all the variables with subscripts' $n+1$ are the unknowns. Applying these numerical approximations to equations (1) and (2) yields:

$$C\, y_j^{n+1} + D\, Q_j^{n+1} + E\, y_{j+1}^{n+1} + F\, Q_{j+1}^{n+1} + G = 0 \tag{6}$$

$$C'\, y_j^{n+1} + D'\, Q_j^{n+1} + E'\, y_{j+1}^{n+1} + F'\, Q_{j+1}^{n+1} + G' = 0 \tag{7}$$

Where $C, D, E, F, G, C', D', E', F'$, and G' are coefficients computed with known values at time level n. Equations (6) and (7) constitute a system of linear algebraic equations in four unknowns. As there are J points on the row $n+1$, there are $J-1$ rectangular grids and $J-1$ cells in the channel. Thus there are $2(J-1)$ equations for the evaluation of $2J$ unknowns. Two boundary conditions provide the necessary two additional equations to close the system. Any standard method of solving linear algebraic equations can be applied to get the solution of $2(J-1)$

equations. The double-sweep method [4,7] is very efficient and saves the time consumed by solution.

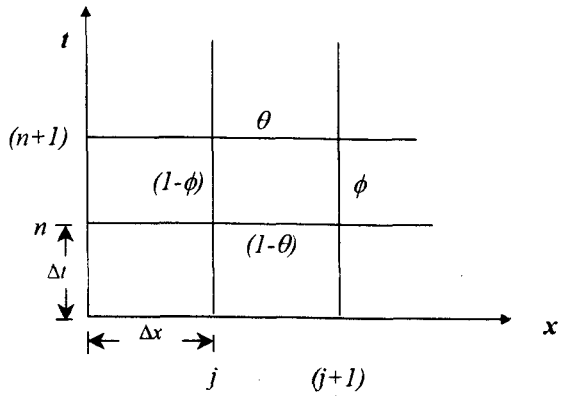

Fig. 1. Computational Grid for Preissmann Scheme

Inverse Explicit Scheme

For operation problems, the expected discharge and water level downstream boundary conditions are specified. The inverse explicit scheme is an explicit solution based on the Preissmann scheme. Considering the time level *(N)* as the final condition, Fig. 2, and knowing Q_J, and y_J between any two time levels at the downstream section, the discharge and water depth profile at the time level *(N-1)* can be computed by proceeding first backward in time and then backward in space. In this approach, the Preissmann scheme, Fig. 2, is written as:

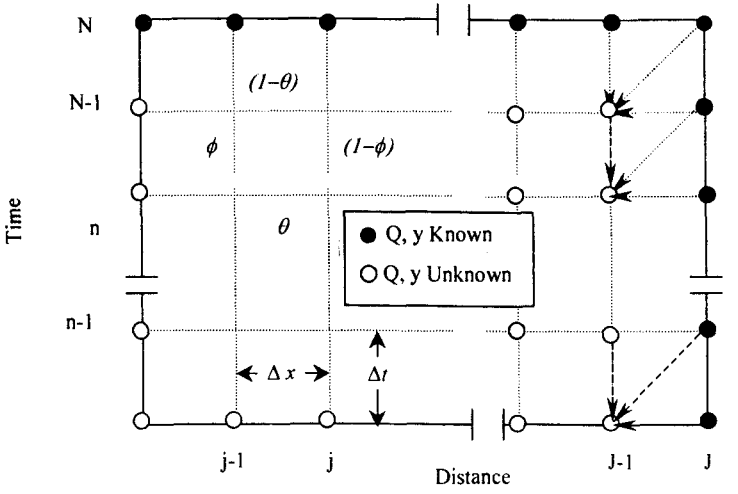

Fig. 2. Inverse Explicit Computational Grid

$$\frac{\partial f}{\partial t} = \phi \frac{f_{j-1}^{n} - f_{j-1}^{n-1}}{\Delta t} + (1-\phi) \frac{f_{j}^{n} - f_{j}^{n-1}}{\Delta t} \tag{8}$$

$$\frac{\partial f}{\partial x} = \theta \frac{f_{j}^{n} - f_{j-1}^{n}}{\Delta x} + (1-\theta) \frac{f_{j}^{n} - f_{j-1}^{n}}{\Delta x} \tag{9}$$

$$f(x,t) = \theta\left[\phi f_{j-1}^{n} + (1-\phi) f_{j}^{n-1}\right] + (1-\theta)\left[\phi f_{j-1}^{n} + (1-\phi) f_{j}^{n}\right] \tag{10}$$

The solution begins at the top-right corner of the time-distance plane, Fig. 2. The application of the finite difference equations yields an algebraic system of two equations and two unknowns. The solution obtained cell by cell, moving first backward in time and then backward in space.

DESCRIPTION OF TEST CANAL

The performance of the inverse explicit finite difference scheme was tested using the example presented in Liu, et al. 1992 [6]. The foregoing test is for unsteady flow in a trapezoidal channel with a bottom width of *5.0m* and side slopes *1.5H to 1V*. The bottom slope is *0.001*, Manning's $n = 0.025$, the channel length is *2.5 km*, and a fixed overflow weir with free flow condition is considered as a downstream outlet. At the downstream outlet, the discharge increases from *5* m^3/sec to *10* m^3/sec in one hour, it remains constant at *10* m^3/sec for the next two hours, then decreases to *5.0* m^3/sec in one hour (demand line in Fig. 3.). The discharge-water depth relationship of a fixed weir under free-flow conditions was used to obtain the water depth at the downstream end section. The discharge and water depth at the upstream intake, Figs. 3 and 4, were computed using the specified discharge and water depth at the downstream end section as the initial conditions.

The obtained upstream discharge hydrograph was then used as upstream boundary condition and the fixed overflow weir at the end of the channel was used as the downstream boundary condition, to simulate the flow in the channel with the routing implicit finite difference scheme. The computed downstream hydrographs reasonably reproduced the prescribed demand, Figs. 3 and 4.

NUMERICAL TESTS AND COMPARISON OF RESULTS

The computed upstream discharge and depth hydrographs using both the inverse explicit scheme and the inverse implicit scheme are shown in Figs. 3 and 4. The space interval $\Delta x = 100\ m$ and time interval $\Delta t = 200\ sec$ were used in both the inverse explicit method and the inverse implicit method. The weighting coefficient $\phi = 0.5$ and the weighting coefficient $\theta = 1.0$ were used in the inverse explicit method while the weighting coefficient $\phi = 1.0$ and the weighting coefficient $\theta = 0.6$ were used in the inverse implicit method. The computed results using the inverse explicit scheme showed approximately the same accuracy as the corresponding results obtained by the inverse implicit scheme, Figs. 3 and 4. The upstream discharge hydrograph obtained by the

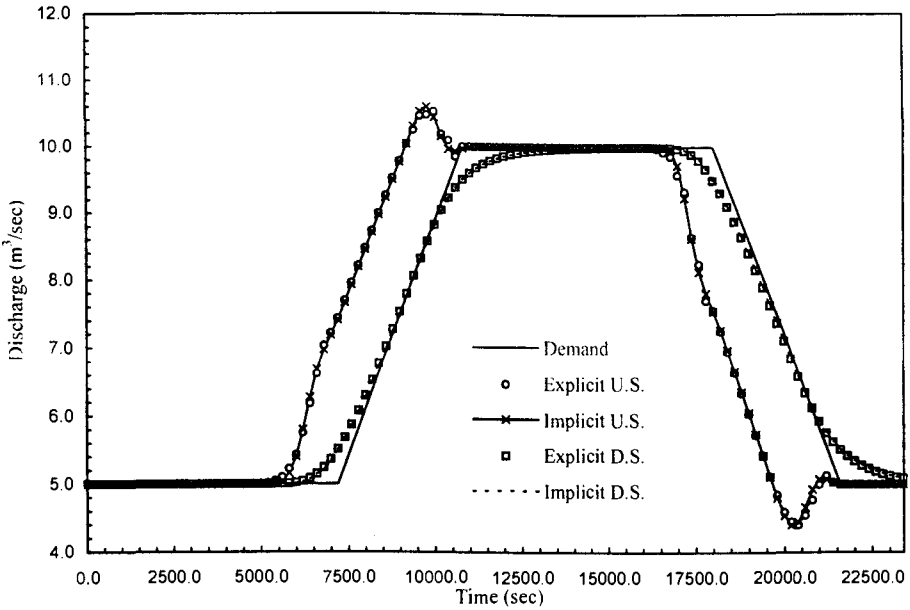

Fig. 3. Comparison between Discharge Hydrographs Using Inverse Explicit Method and Inverse Implicit Method.

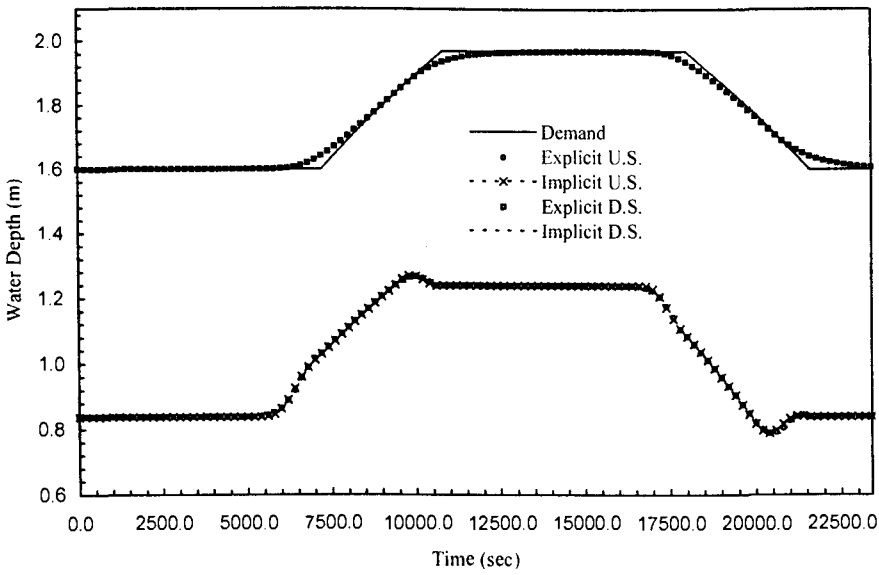

Fig. 4. Comparison between Water Depth Hydrographs Using Inverse Explicit Scheme and Inverse Implicit Scheme.

inverse explicit scheme, when used as upstream boundary conditions in the routing problem, reproduced approximately the same downstream flow hydrographs as the corresponding hydrographs obtained using the inverse implicit scheme. Also, the reproduced computed downstream hydrographs were close to what are expected, Figs. 3 and 4.

The inverse explicit scheme was tested with numerical experiment by verifying the following parameters: the computation space interval Δx, the time interval Δt, the weighting coefficient ϕ, and the weighting coefficient θ. All these parameters were being constant except one of them which could be tested in sequence. The space interval $\Delta x = 100$ *m*, the time interval $\Delta t = 200$ *sec*, the weighting coefficient $\phi = 0.5$, and the weighting coefficient $\theta = 1.0$ were kept constant in the computation of upstream hydrographs, except for the tested parameter.

The computed upstream hydrographs using $\Delta x = 50$ *m, 100 m*, and *250 m* are illustrated in Figs. 5 and 6. As shown in Figs. 5 and 6, the effect of the space interval on the computed upstream hydrographs and the reproduced downstream hydrographs has a negligible influence which could be confirmed by Liu et al. 1992 [6].

The computed upstream hydrographs, using $\Delta t = 200$ *sec, 600 sec*, and *1200 sec* are shown in Figs.7 and 8. The result of the time interval $\Delta t = 200$ *sec* shows more oscillation in the computed results during both the increasing and decreasing of the flow rate than that of the bigger values. Liu et al. 1992 [6] mentioned that the computed upstream hydrographs using the backward operation explicit method with a smaller time interval has more oscillation which can cause the failure of the computation. It is known that the application of the explicit schemes in the routing problems required small time intervals to coincide with the Courant condition. In the contrary to this, Figs. 7 and 8 show that the computed upstream hydrographs becomes smoother with larger time intervals. The accuracy of the reproduced downstream hydrographs is better for smaller time interval than those obtained using bigger time intervals. So, with smaller time interval, the computed upstream inflow can be defined more accurately, but this will produce more oscillation to meet more specifications of the downstream outflow.

The computed upstream hydrographs for different values of the weighting coefficient θ show that the stability is improved when θ increases from *0.8* to *1.0*. Figs. 9, and 10 show the computed upstream hydrographs for $\theta = 0.8, 0.9$, and *1.0*. Liu et al. 1992 [6] showed a very big oscillation occurred on the upstream computed hydrographs, using the backward operation explicit method, for $\theta = 0.6$. This oscillation was damped as θ increased from *0.6* to *1.0*.

As shown in Figs. 11 and 12, the effect of the weighting coefficient ϕ on the computed upstream hydrographs and the reproduced downstream hydrographs could be neglected. Liu et al. 1992 [6] didn't test the effect of the weighting coefficient ϕ on the computed hydrographs using the backward-operation

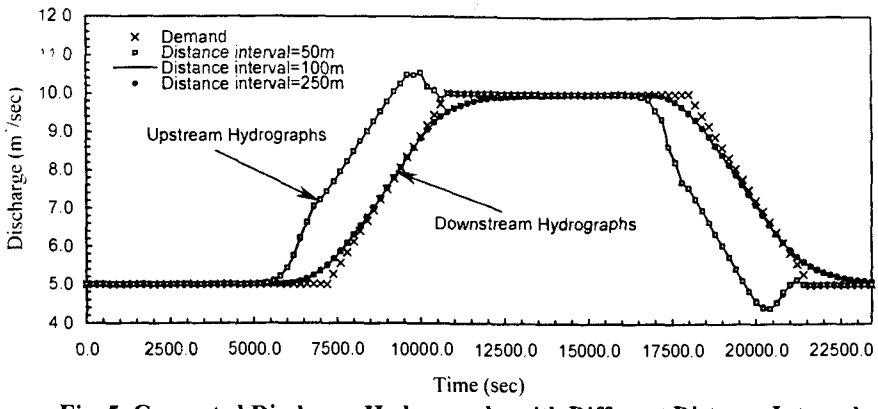

Fig. 5. Computed Discharge Hydrographs with Different Distance Intervals.

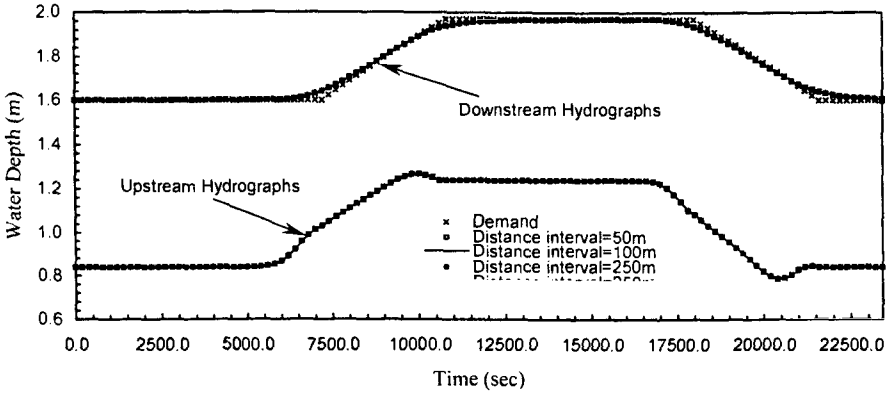

Fig. 6. Computed Water Depth Hydrographs with Different Distance Intervals.

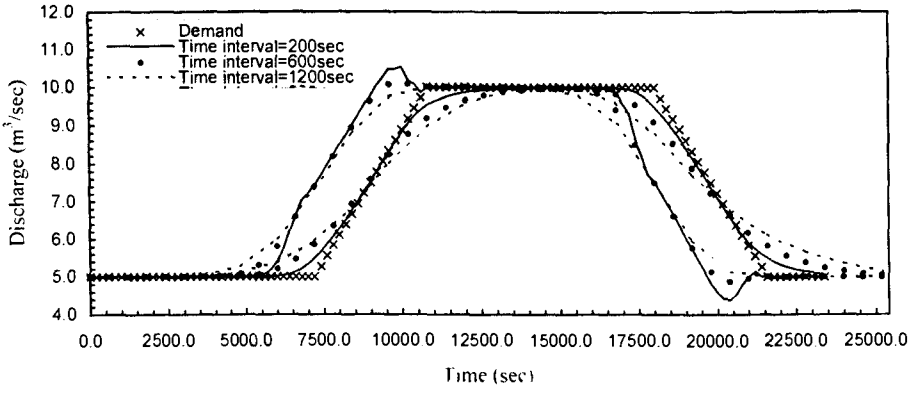

Fig. 7 Computed Discharge Hydrographs at Different Time Intervals.

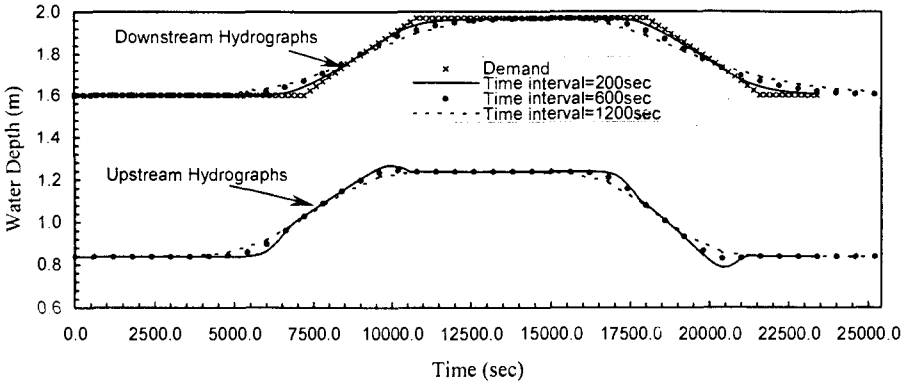

Fig. 8. Computed Water Depth Hydrographs at Different Time Intervals.

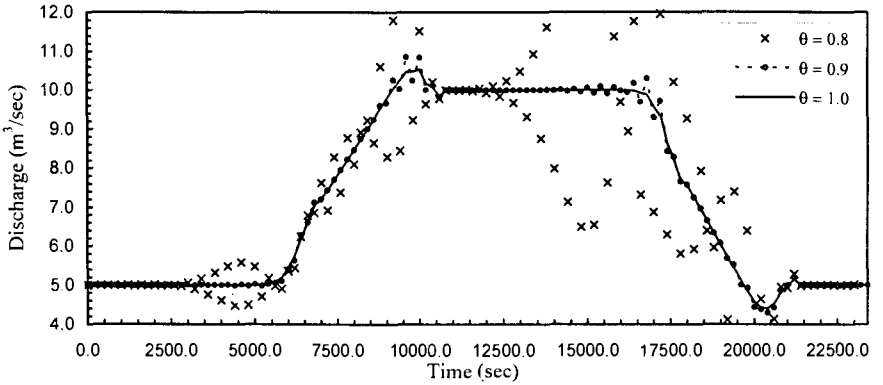

Fig. 9. Computed Upstream Discharge Hydrographs with Different θ Factors.

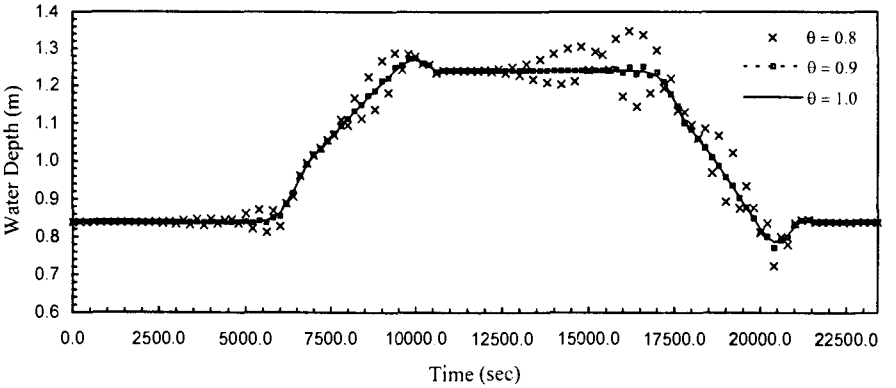

Fig. 10. Computed Upstream Water Depth Hydrographs with Different θ Factors.

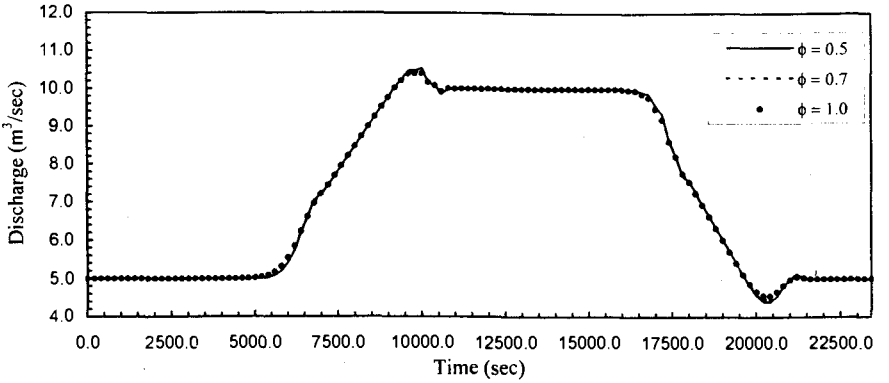

Fig. 11. Computed Upstream Discharge Hydrographs with Different ϕ Factors.

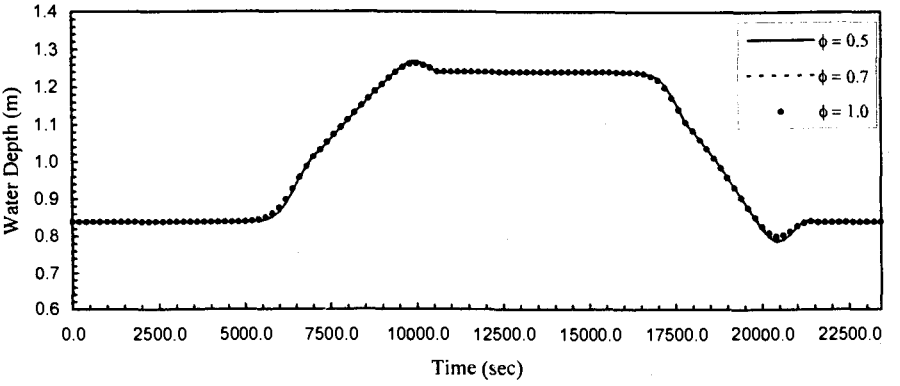

Fig. 12. Computed Upstream Water Depth Hydrographs with Different ϕ Factors.

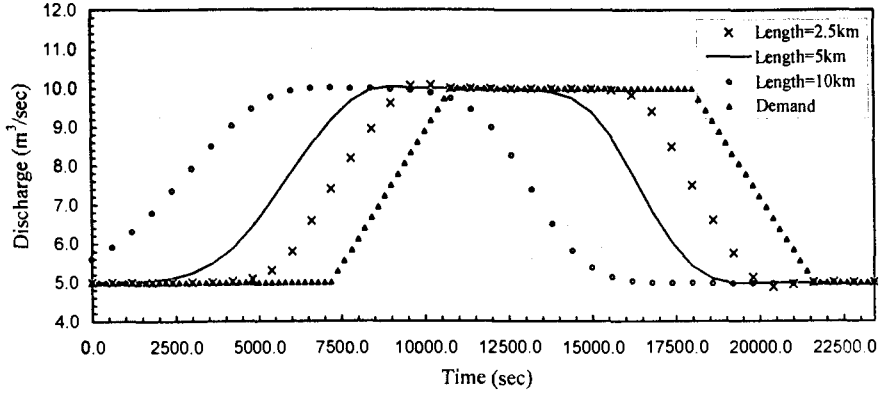

Fig. 13. Computed Upstream Discharge Hydrographs for Different Canal Lengths.

The inverse explicit finite difference scheme was also tested using different channel length. The space interval $\Delta x = 100\ m$, the time interval $\Delta t = 600\ sec$, the weighting coefficient $\phi = 0.5$, and the weighting coefficient $\theta = 1.0$ were used in the computation. As shown in Figs. 13 and 14, the length of the channel doesn't affect the oscillations of the computed upstream hydrographs, but the computed upstream hydrographs are more shifted to the left, as the channel length increases, to provide the same downstream flow pattern. Liu et al. 1992 [6] mentioned that the oscillations in the computed upstream discharge hydrographs using the backward operation explicit method are amplified with the increasing of channel length.

The effect of Manning's roughness coefficient on the upstream hydrographs for a channel length of 2.5 *km* and a bottom slope of *0.001* was tested using n=*0.025, 0.02, and 0.015*. The space interval $\Delta x = 100\ m$, the time interval $\Delta t = 600\ sec$, the weighting coefficient $\phi = 0.5$, and the weighting coefficient $\theta = 1.0$ were used in the computation. The computed upstream discharge hydrograph shifts to the left as the Manning's roughness coefficient increases to provide the same downstream flow pattern. The computed upstream depth hydrograph shifts upward and to the left as the Manning's roughness coefficient increases. The results are shown in Figs. 15 and 16.

MODEL APPLICATION TO NON-PRISMATIC CHANNEL

The finite difference Preissmann implicit scheme of El-Mansouria canal, between Sanayet regulator and Bahr Tanah, was calibrated to give simulated hydrographs very close to the measured hydrographs [10]. The inverse explicit finite difference scheme was applied to this reach of El-Mansouria canal. The length of this reach is *18 km*, the cross section spacing is *2.0 km*, the channel bed slope is 4.5 *cm/km*, and the shape of the cross section is irregular [10]. The value of Manning's roughness coefficient $n = 0.025$ gave a good agreement between measured and computed hydrographs at a calibrated point *6 km* downstream from Sanayat regulator, Figs. 17 and 18. When a high level of calibration can be achieved and verified, then it may be possible to extent the application of the model beyond the limits of calibration [4,7]. The computed discharge hydrographs using the inverse explicit scheme were compared with those obtained using the inverse implicit scheme as illustrated in Fig. 19. At the downstream section, the discharge increases from $50\ m^3/sec$ to $55\ m^3/sec$ in one hour, it remains constant at $55\ m^3/sec$ for two hours, then decreases to $50\ m^3/sec$ in the next hour (demand line in Fig.19). The space interval $\Delta x = 2000\ m$, the time interval $\Delta t = 1800\ sec$, the weighting coefficients $\phi = 0.5$, and $\theta = 1.0$, were used in the computations of the inverse explicit scheme. In the computation of the inverse implicit scheme, the space interval $\Delta x = 2000\ m$, the time interval $\Delta t = 600\ sec$, the weighting coefficients $\phi = 1.0$, and $\theta = 0.6$ were used. As shown in Fig. 19, there is small difference between the computed upstream discharge hydrographs using both the inverse explicit scheme and the inverse implicit scheme. The time interval $\Delta t = 1800\ sec$ was used in the computation of

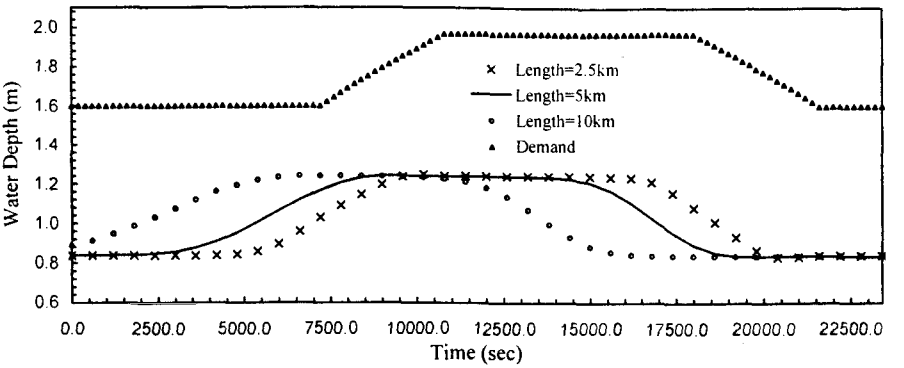

Fig. 14. Computed Upstream Water Depth Hydrographs for Different Canal Lengths.

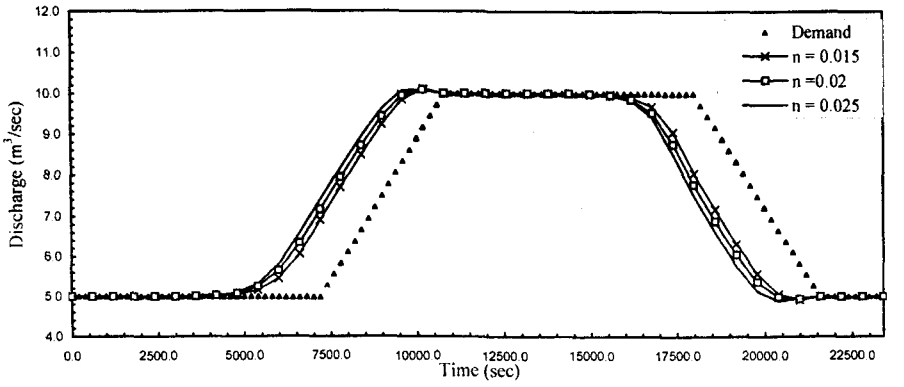

Fig. 15. Computed Upstream Discharge Hydrographs for Different Manning's Roughness coefficient.

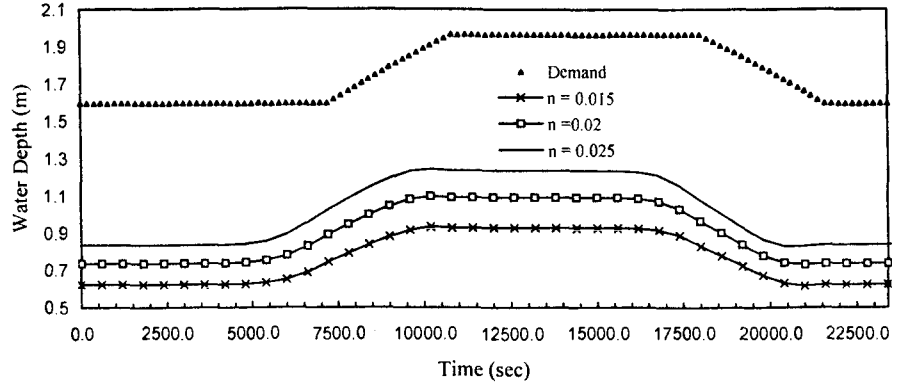

Fig. 16. Computed Upstream Water Depth Hydrographs for Different Manning's Roughness Coefficient

the inverse explicit scheme to reduce the oscillation of the computed upstream hydrograph. The damping effect of the finite difference schemes is visible as shown in the computed hydrographs, Figs. 17 and 19, due to the mild slope of the canal. The computed upstream discharge hydrographs using the applied schemes, when used as upstream boundary conditions in the calibrated finite difference implicit routing scheme of El-Mansouria canal, reproduced approximately the same downstream discharge hydrographs. Also, the reproduced downstream hydrographs were close to the demand line, Fig. 19.

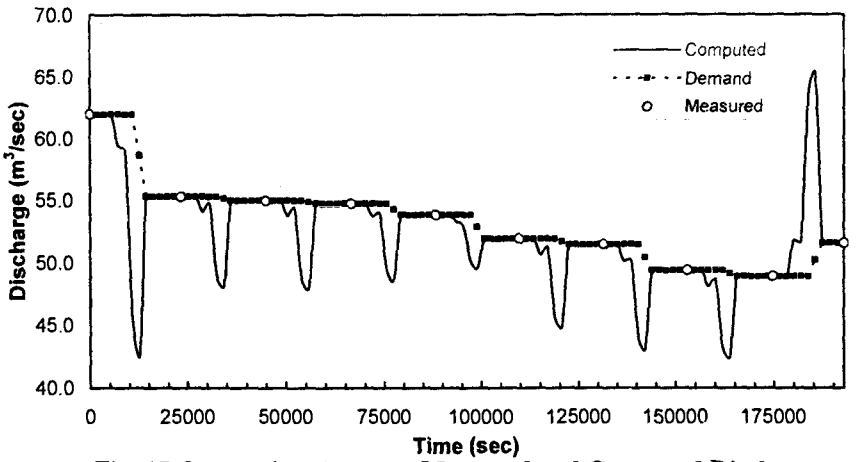

Fig. 17.Comparison between Measured and Computed Discharge Hydrographs at The Measured Station.

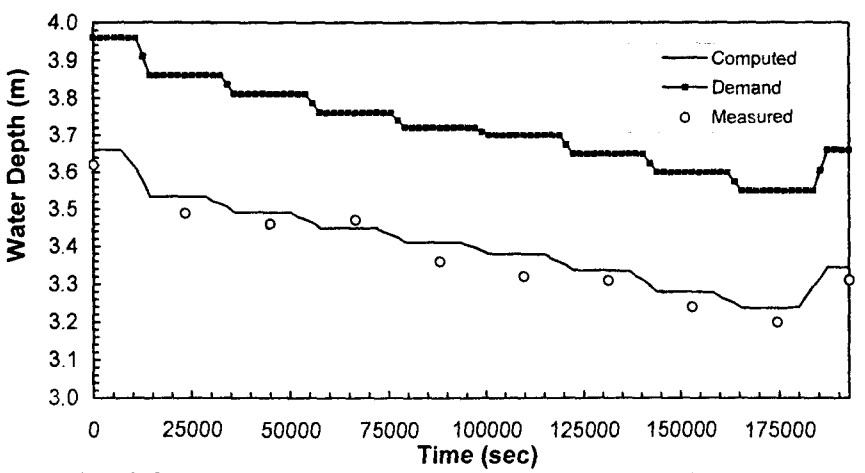

Fig. 18.Comparison between Measured and Computed Water Depths Hydrographs at The Measured Station.

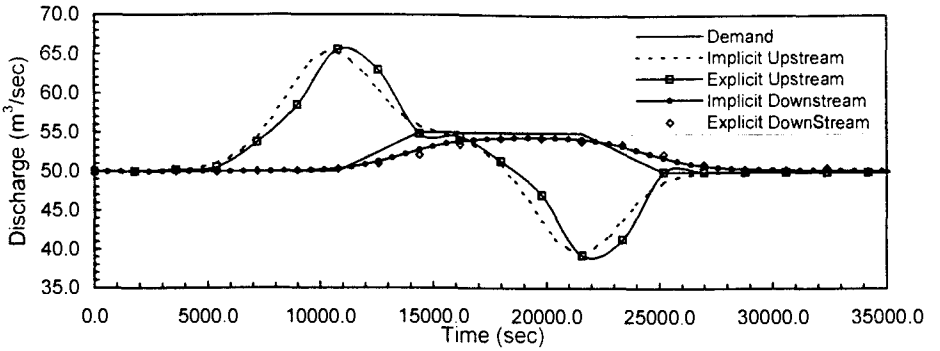

Fig. 19. Comparison between Computed Discharge Hydrographs for El-Mansouria Canal Using Inverse Implicit Scheme and Inverse Explicit Scheme.

CONCLUSIONS

Unsteady flow problems in open channels can be classified into two types: routing and operation-type problems. The routing problem is used to predict the discharge and water level in the channel during the future time series under the given conditions. On the other hand, the operation problem is used to compute the inflow at the upstream section of the channel or a schedule of operation for the regulating structures of the delivery system to get a predefined water demand at the downstream end of the channel.

A finite difference algorithm for regulating unsteady flow in open channel has been presented. The method is explicit and numerically stable. It can be used to define the upstream inflow and setting of controlling structures according to the required downstream outflow. The inverse explicit scheme was tested with the following parameters: the space interval Δx, the time interval Δt, the weighting coefficient ϕ, and the weighting coefficient θ.

The effect of the computational space interval on the computed upstream hydrographs and the reproduced downstream hydrographs could be neglected for the used values of Δx. The computed results, using the inverse explicit scheme, $\Delta t \leq 200$ sec, may show oscillations especially in a long channel with small computing time interval. The oscillations increases with the decreasing value of the time interval, although the accuracy of computed results increases with decreasing of time interval. The effect of the weighting coefficient ϕ on the computed upstream hydrographs and the reproduced downstream hydrographs is negligible. The oscillations of the computed upstream hydrographs were damped when θ increases from *0.8* to *1.0*.

The length of the channel didn't affect the oscillations of the computed upstream hydrographs using the inverse explicit scheme with bigger computational time interval, $\Delta t = 600$ *sec*. The computed upstream hydrographs shift more to the left as the channel length increases to provide the same

The effect of Manning's roughness coefficient on the computation of upstream hydrographs was tested. The computed upstream discharge hydrograph shifts to the left as the Manning's roughness coefficient increases to provide the same downstream flow pattern. The computed upstream water depth hydrograph shifts upward and to the left as the Manning's roughness coefficient increases.

The inverse explicit finite difference scheme was applied successfully, using time interval, $\Delta t = 1800$ *sec,* to a non-prismatic reach of El-Mansouria canal between Sanayet regulator and Bahr Tanah canal.

The computed results using the inverse explicit scheme with appropriate weighting coefficients ($\theta = 1.0$, $\phi = 0.5$) show the same accuracy as that obtained using the inverse implicit scheme . All the inverse solutions, when used as upstream boundary condition to the routing model, reproduced downstream flow hydrographs very close to the required outflow hydrographs.

REFERENCES

1. Abbott, M. B., "Computational Hydraulics; Elements of The Theory of Free Surface Flows", Pitman Publishing Limited, London, 1979.
2. Bautista, E., Clemmens, A.J., and Strelkoff, T. ," Comparison of Numerical Procedures for Gate Stroking", Journal of Irrigation and Drainage Engineering, ASCE, Vol.123, No.2, pp. 129-136, March/April,1997.
3. Chaudhry, M.H., "Open-Channel Flow", Prentice Hall, Inc., New Jersey, USA, 1993.
4. Cung, J.A., Holly, F.M. and Verwey, J.A. , "Practical Aspects of Computational River Hydraulics", Pitman Publishing Limited, London, 1980.
5. Schuurmans, W., "A Model to Study The Hydraulic Performance of Controlled Irrigation Canals", The Center for Operational Water Management, Delft University of Technology, 1991.
6. Liu, F., Feyen, J., and Barlamont, J., " Computational Method for Regulating Unsteady Flow in Open Channels.", Journal of Irrigation and Drainage Engineering, ASCE,Vol.118, No.10, pp. 674-689, September/October,1992.
7. Mahmood, K., and Yevjevich, "Unsteady Flow in Open Channels", Vol. I, Water Wylie, E. Resources Publications, 1975.
8. Reddy, J.M., Dia, A., and Oussou, A., "Design of Control Algorithm for Operation of Irrigation Canals", Journal of Irrigation and Drainage Engineering, ASCE,Vol.118, No.6, pp. 852-867, November/December,1992.
9. Rogers, D., and Goussard, J., "Canal Control Systems Currently in Use", Journal Irrigation and Drainage Engineering, 124(1),11-15, 1998.
10. Shamaa, M. T., "Application of Resistance Formulae in Irrigation Canals", M.Sc. Thesis, Civil Engineering Dept., El Mansoura University, Egypt, 1989.
11. Shamaa, M. T., "A Comparative Study of Two Numerical Methods for Regulating Unsteady Flow in Open Channels", Mansoura Engineering Journal, Volume 27, No.4, December 2002.
12. Wylie, E. B., "Control of Transient Free Surface Flow" Journal of Hydraulic

NOTATION

The following symbols are used in this paper:

A = wetted cross-sectional area;
b = wetted top width;
f = general function;
g = gravitational constant;
j = cross-section index;
n = time-level index; Manning's coefficient;
Q = discharge (through A);
S_0 = bottom slope of the channel;
S_f = friction slope;
t = time;
x = space;
y = depth of flow ;
Δt = time interval;
Δx = space interval;
ϕ = a weighting coefficient for distributing terms in space; and
θ = a weighting coefficient for distributing terms in time.